

Reflected entropy in an evaporating black hole through non-isometric map

Bin Chen,^{1,2,3} Zhi-jun Yin²

¹*Institute of Fundamental Physics and Quantum Technology,
& School of Physical Science and Technology,
Ningbo University, Ningbo, Zhejiang 315211, China*

²*School of Physics, Peking University, No.5 Yiheyuan Rd, Beijing 100871, P.R. China*

³*Center for High Energy Physics, Peking University, No.5 Yiheyuan Rd, Beijing 100871,
P. R. China*

chenbin1@nbu.edu.cn, yinzhijun@stu.pku.edu.cn

ABSTRACT: The black hole information paradox has been an important problem in quantum gravity. In the study of evaporating black hole, it has been proposed that the holographic map between the semi-classical effective description in bulk and the fundamental description in boundary cannot be isometric. In this work, we would like to study the reflected entropy in an evaporating black hole model through non-isometric holographic map. We assume that the evaporating is slowly enough that it makes sense to ascribe a slowly varying temperature to the Hawking radiation. We then introduce a two-sided black hole model to canonically purify the semi-classical state. The holographic map to the fundamental description is non-isometric and defined by a Haar random unitary matrix. We show that the entropy of radiation in the model computed in the fundamental description matches the result read from the quantum extremal surface formula and agrees with the Page curve. Furthermore, through non-isometric holographic map, we study the reflected entropies between different regions, including the one between the black holes on different sides, the one between the radiations distributed symmetrically but disconnectedly, and the one between the black hole and the radiation on single side. Our results are consistent with the existing ones based on the effective descriptions.

Contents

1	Introduction	1
2	A model for two-sided black hole	4
2.1	Two-sided black hole model	5
2.2	Averaging and the Haar integral	6
3	Reflected entropy	10
3.1	Reflective entropy between black holes	11
3.2	Reflective entropy between radiations	17
3.3	Radiation and black hole	20
4	Conclusion and discussion	22

1 Introduction

One important implication of AdS/CFT correspondence [1] is that the black hole evaporation process must keep the unitarity. The entropy of Hawking radiation is an important physical quantity for detecting whether black hole evaporation is unitary or not. If black hole evaporation is unitary, the entropy of Hawking radiation should follow the Page curve [2, 3]. In the AdS/CFT correspondence, the boundary entropy and its bulk dual, the quantum extremal surface (QES) formula [4], when applied to evaporating black holes, will lead to the so-called “island rule” [5–11], which helps to show that the entropy of Hawking radiation obeys the Page curve.

The quantum extremal surface has also been used to study the problem of bulk reconstruction, which involves representing bulk operators in the Hilbert space of the boundary CFT [12–18]. During the research, it was found that the problem of bulk reconstruction can be discussed within the framework of quantum error correction [19–22]. The underlying key points are as follows. The Hilbert space of the low-energy effective field theory in the bulk can be mapped to the boundary Hilbert space by an approximate isometric map $V : \mathcal{H}_{bulk} \rightarrow \mathcal{H}_{boundary}$ (an isometry is a linear map satisfying $V^\dagger V = I$). In the language of quantum error correction, \mathcal{H}_{bulk} is the “logical” Hilbert space, and $\mathcal{H}_{boundary}$ is the “physical” Hilbert space. If the boundary Hilbert space can be tensor factorized into two parts $\mathcal{H}_{boundary} = \mathcal{H}_A \otimes \mathcal{H}_{\bar{A}}$, then the bulk can

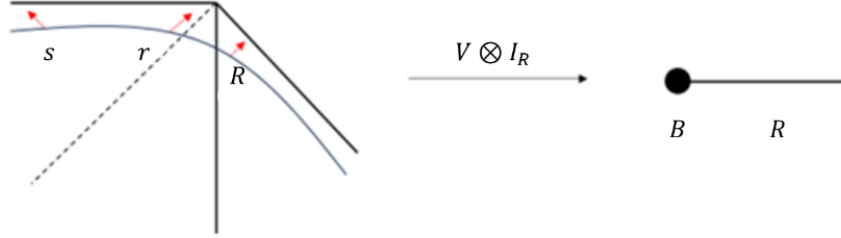


Figure 1. Holographic map of a single-sided black hole coupled with the radiation R . The s modes, the r modes, and the R modes in the radiation region appear on the selected Cauchy surface in the effective description.

be decomposed along the corresponding quantum extremal surface X_A^{\min} into $\mathcal{H}_{\text{bulk}} = \mathcal{H}_a \otimes \mathcal{H}_{\bar{a}}$. In this case, for the bulk density operator ρ , we have the QES formula:

$$S(\text{tr}_{\bar{A}}(V\rho V^\dagger)) \approx \frac{\text{Area}(X_A^{\min})}{4} + S(\rho_a). \quad (1.1)$$

Strictly speaking, the above bulk reconstruction only applies to the emergence of spacetime outside the blackhole horizon.

The above holographic map encounters serious problems in describing the spacetime behind the blackhole horizon. For example, in the late stage of black hole evaporation, the degrees of freedom in the bulk effective field theory will vastly exceed the degrees of freedom on the boundary. On the one hand, as a simple model, one may take the black hole as a quantum system B with Hilbert space \mathcal{H}_B containing the microscopic degrees of freedom of black hole, coupled to a “reservoir” R with Hilbert space \mathcal{H}_R . The Hawking radiation from the black hole can propagate out into the reservoir. In this so-called *fundamental* description, the quantum system could belong to a high-energy band of holographic CFT, and the reservoir R could be a kind of free-field theory on a half-space in one higher dimension than the holographic CFT if we may ignore the interaction of radiations safely. On the other hand, from the bulk effective field theory perspective, there are two kinds of modes inside the black hole: one kind of modes consists of the states falling into the black hole, denoted as s , and the other kind of ones denoted as r are entangled with the Hawking radiations. The semi-classical bulk description is referred to as the *effective* description. The holographic map in this case is defined as

$$V \otimes I_R : \mathcal{H}_s \otimes \mathcal{H}_r \otimes \mathcal{H}_R \rightarrow \mathcal{H}_B \otimes \mathcal{H}_R, \quad (1.2)$$

as shown in Fig. 1. Here the interactions between two kinds of modes have been neglected. At the late stage of black hole evaporation, the entanglement entropy of the

radiations in the effective description far exceeds the entropy of the black hole,

$$S(\rho_r) = S(\rho_R) \gg \log |B|. \quad (1.3)$$

In other words, the dimension of the Hilbert space \mathcal{H}_r is much larger than that of \mathcal{H}_B , $|r| \gg |B|$. Therefore, the linear map $V : \mathcal{H}_s \otimes \mathcal{H}_r \mapsto \mathcal{H}_B$ must be non-isometric, and a large number of null states in the effective description will be annihilated by the map. In [23], the authors constructed a non-isometric holographic map from the effective description to the fundamental description and proved that it has properties such that observing the null states requires the operations of exponential complexity. It was showed that these non-isometric codes protected by computational complexity could explain the emergence of the black hole interior.

The model in [23] was refined in [24] by taking into account of the energy conservation and the thermal nature of the Hawking radiation. In [24], it was assumed that the black hole evaporates slowly enough that it makes sense to ascribe a slowly varying temperature to the Hawking radiation. In this so-called quasi-adiabatic regime, Hawking's derivation is valid, and it requires that $S_{BH} \gg c$, where c is the degrees of freedom of massless modes. More precisely, the black hole is assumed to evaporate in a series of time steps whose sizes are of the order of the scrambling time of the black hole. In this picture, the black hole evolves approximately through a sequence of microcanonical states, and the semi-classical state is now a thermofield double with a slowly varying temperature. One may canonically purify the thermofield double state by considering the two-sided black hole. In this setup, one may discuss richer physics[8, 25, 26]. Now the entire system is naturally divided into multiple regions, we can study the entanglements between these regions. In this work, we plan to study the reflected entropy in this two-sided black hole model.

The reflected entropy was first introduced in the study of canonical purification for the entanglement wedge cross-section[27], and has been under intensive study in various situations, including holographic models[28–47], random tensor networks[48–51], the free scalar and fermion field theories[52–55], Chern-Simons theory[56–58], conformal field theory[59–63], Lifshitz theory[64], etc. The reflected entropy is a probe of tripartite entanglement [65, 66]. It is remarkable that even though the monotonicity of the reflected entropy gets lost for certain quantum state[67] and for the ground state in free Lifshitz field theories[64], it holds for holographic state[27], as the consequence of the “entanglement wedge nesting” property.

We are going to compute the reflected entropies between different regions in the two-sided black hole model. Our study is in spirit similar to the one appearing in the 2D eternal black hole plus CFT model [30, 31], where the two-sided black hole was used to discuss the thermal equilibrium between the black hole and the thermal bath [8].

We will calculate the reflected entropy between the black holes on different sides, the one between the radiations distributed in a symmetric but disconnected way, and the one between black hole and the radiations. In the case at hand, we verify the equality between the reflected entropy between the black hole and the radiation in the single-sided black hole model and the entanglement entropy of radiations in the two-sided black hole model, despite the fact that two models have different holographic maps. To obtain analytical results, we focus on the high-temperature limit, where the system can be taken as the microcanonical ensemble. In this case, we can clearly observe the changes in reflected entropy during the black hole evaporation process.

The remaining parts of the paper are organized as follows. In Section 2, we introduce briefly the two-sided black hole. In Section 3, we compute the reflected entropies and the mutual information between different regions. We end with conclusion and discussion in Section 4.

2 A model for two-sided black hole

We first review briefly the model in [23]. In this model, to achieve the non-isometry of the holographic map, we consider a larger Hilbert space $\mathcal{H}_s \otimes \mathcal{H}_r \otimes \mathcal{H}_f$, where f are some extra degrees of freedom such that:

$$|f||s||r| = |P||B|. \quad (2.1)$$

For a positive integer $|P|$, there is a tensor decomposition of the Hilbert space

$$\mathcal{H}_s \otimes \mathcal{H}_r \otimes \mathcal{H}_f = \mathcal{H}_B \otimes \mathcal{H}_P. \quad (2.2)$$

The holographic map is defined as

$$V \equiv \sqrt{|P|} \langle 0|_P U |\psi_0\rangle_f, \quad (2.3)$$

where $|\psi_0\rangle_f$ is a fixed quantum state on \mathcal{H}_f , $|0\rangle_P$ is a fixed quantum state on \mathcal{H}_P , and U is a unitary operator on $\mathcal{H}_s \otimes \mathcal{H}_r \otimes \mathcal{H}_f$, which satisfies the statistical properties of being Haar random. The coefficient $\sqrt{|P|}$ is used for normalization. We can regard $|\psi_0\rangle_f$ as describing any extra effective-field-theory degrees of freedom we are not interested in. This model achieves the non-isometry of the holographic map through the post-selection on the unitary operator by $\langle 0|_P$.

For an evaporating black hole, the r modes form maximally entangled pairs with the radiations [68]. Ignoring the contribution of $|\psi_0\rangle_f$, we consider that the black hole is formed by the infalling s state. From this, we can find that $|P| = |r||R|$, $|0\rangle_P = |\text{MAX}\rangle_{rR}$ is the maximal entangled state on $\mathcal{H}_r \otimes \mathcal{H}_R$ [23, 24]. So we can derive the form of the holographic map:

$$V = \sqrt{|r||R|} \langle \text{MAX}|_{rR} U. \quad (2.4)$$

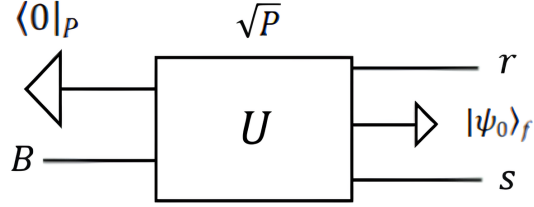


Figure 2. The diagram of the holographic map V , in which U is a unitary operator and the external legs on both sides correspond to the degrees of freedom of the respective Hilbert spaces. The degrees of freedom of f and P are fixed by $|\psi_0\rangle_f$ and $\langle 0|_P$. For clarity, the order of the external leg indices in the diagram matches the indices of U in (2.8), i.e., the left side corresponds to the index i , and the right side corresponds to the index j .

2.1 Two-sided black hole model

Next, let us discuss the case of a two-sided black hole. Typically, in AdS/CFT, without matter and evaporation, a black hole is dual to a mixed state in the CFT. In the simplest setting, a static black hole in AdS is dual to a thermal state in CFT. And a two-sided black hole is dual to the purification of this mixed state, the so-called thermal-field double state, in two copies of the conformal field theory[25]. Here we generalize the picture to take into account the radiations. We assume that the radiation is slow enough such that we can approximately take the black hole as a state in (quasi)-thermal equilibrium. In our model, the infalling state s under the effective description corresponds to the formation process of the black hole. We assume it to be varying very slowly as well such that it does not change the mass of the black hole quickly. It could be a mixed state or a pure state. In any case, we may have a copy s' of the infalling state s to purify s , with the pure state composed of s and s' being denoted as $|S\rangle_{ss'}$.

We consider the coupling of a two-sided black hole with the radiations R and R' on two sides. In the fundamental description, we have to doubly copy the CFT and the reservoir, as shown in Fig. 3. At this point, the modes r and r' form maximally entangled states with the modes R and R' , respectively, denoted as $|X\rangle_{rR}$ and $|X'\rangle_{r'R'}$. In the effective description, the quantum state of the system is taken as

$$|\psi\rangle = |X\rangle_{rR} |X'\rangle_{r'R'} |S\rangle_{ss'}. \quad (2.5)$$

Now the holographic map is as shown in figure 3. If we regard s and s' , r and r' , B and B' respectively as the double copy of the former Hilbert space in (2.2), following

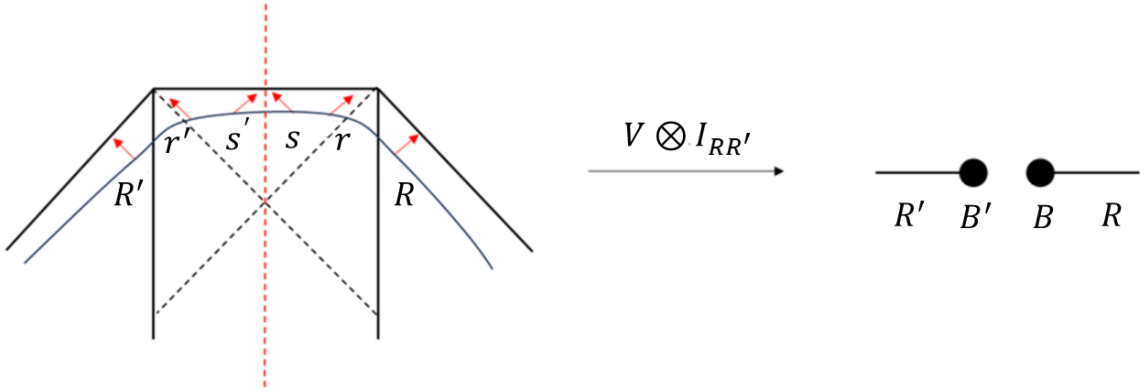


Figure 3. The holographic map of the model in which a two-sided black hole is coupled with the radiations on two sides. On the left side, the effective description is obtained by doubly copying a single-sided evaporating black hole along the red dashed line, resulting in a doubled system. On the right side, the basic description corresponds to the double copies of the quantum system representing the black hole region coupled with the radiation. For the holographic map, the mapping on the radiation regions R and its copy R' are trivial. Similar diagram has been used in the discussions of JT gravity with the radiations at a finite temperature, as shown in [8].

the analysis before, we can define the holographic map as

$$\tilde{V} \equiv |X\rangle\langle \text{MAX}|_{rR}\langle \text{MAX}|_{r'R'}\tilde{U} \quad (2.6)$$

where \tilde{U} is a unitary operator on $\mathcal{H}_s \otimes \mathcal{H}_{s'} \otimes \mathcal{H}_r \otimes \mathcal{H}_{r'}$, which satisfies the statistical properties of being Haar random. For convenience, we set $|X| = |r||r'| = |R||R'|$ and $|Y| = |B||B'|$.

2.2 Averaging and the Haar integral

In the following, we will show how to compute the entropy of radiations in the fundamental description. In our model, for a holographic map \tilde{V} , the corresponding unitary operator \tilde{U} is not a random variable but a fixed value. However, when calculating some quantities with small fluctuations, we can average over \tilde{U} to simplify the computation. Such quantities are referred to as the self-averaging quantities. The Rényi entropy we are going to calculate is a self-averaging quantity. After averaging, we may compute the von Neumann entropy by using the formula

$$S(\rho) = \lim_{n \rightarrow 1} \frac{1}{1-n} \log (\text{tr}(\rho^n)). \quad (2.7)$$

In the calculation, we need to take the average under the Haar measure. The integral under the Haar measure can be generally written as $\int dU f(U, U^\dagger)$ where U and its conjugate transpose U^\dagger are elements of the unitary group $U(N)$, and dU is the Haar measure, satisfying the normalization condition: $\int dU = 1$. In order to obtain non-vanishing integrals under the Haar measure, we need to have the same number of U and U^\dagger . For such integrals, we have:

$$\int dU U_{i_1 j_1} \dots U_{i_n j_n} U^\dagger_{j'_1 i'_1} \dots U^\dagger_{j'_n i'_n} = \sum_{\sigma, \tau \in S_n} \delta_{i_1 i'_{\sigma(1)}} \dots \delta_{i_n i'_{\sigma(n)}} \delta_{j_1 j'_{\tau(1)}} \dots \delta_{j_n j'_{\tau(n)}} \text{Wg}(\sigma \tau^{-1}, N) \quad (2.8)$$

where $\text{Wg}(\sigma \tau^{-1}, N)$ is the Weingarten function[69, 70], and σ and τ are permutations in the symmetric group S_n .

When calculating the n -th Rényi entropy, if n is large, the Weingarten function becomes complex. However, for our model, we usually assume that the degrees of freedom of the black hole and the radiations are large, thus we can assume $N = |X|^2 |Y| \gg 1$. In this case, we can approximate the Weingarten function as

$$\text{Wg}(\pi, N) = \frac{\delta(\pi, e)}{N^n} + O\left(\frac{1}{N^{n+1}}\right) \quad (2.9)$$

where $\delta(\pi, e)$ is the delta function on the group elements in the symmetric group S_n , and e is the identity element. Thus, we can approximate the equation (2.8) as

$$\int dU U_{i_1 j_1} \dots U_{i_n j_n} U^\dagger_{j'_1 i'_1} \dots U^\dagger_{j'_n i'_n} = \sum_{\sigma \in S_n} \frac{1}{N^n} \delta_{i_1 i'_{\sigma(1)}} \dots \delta_{i_n i'_{\sigma(n)}} \delta_{j_1 j'_{\sigma(1)}} \dots \delta_{j_n j'_{\sigma(n)}} + \dots \quad (2.10)$$

Using this approximation, we can easily obtain the n -th Rényi entropy of the radiation region. We can describe the index contraction in $\text{tr}(\rho^n)$ by using a diagrammatic method as shown in Fig. 2. After averaging under the Haar measure, we obtain an integral over the Haar measure multiplied by a coefficient. By calculating these, we can derive the expression for the entropy. The details of the computation is as follows. First, we can simplify the diagram, as shown in Fig. 4. Since $|X\rangle_{rR}|X'\rangle_{r'R'}$ represents the maximally entangled state in the regions rr' and RR' , it can be written as

$$|X\rangle_{rR}|X'\rangle_{r'R'} = \sum_{x=1}^{|X|} \frac{1}{\sqrt{|X|}} |x\rangle_{rr'} |x\rangle_{RR'}. \quad (2.11)$$

For the index contraction on the region RR' , the entanglement is transferred to the contraction of the indices on rr' through the maximally entangled state, and the factors $\frac{1}{\sqrt{|X|}}$ on both sides of the contraction matrix are retained. Thus, after simplifying the

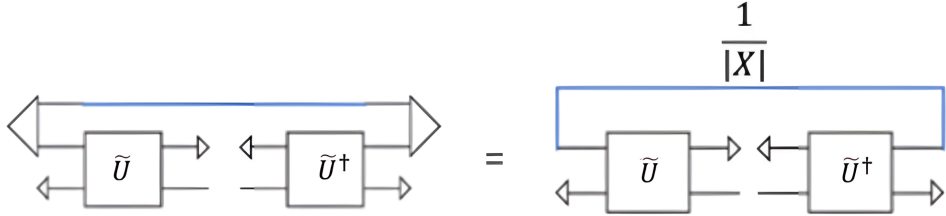


Figure 4. Simplification of the diagram: the blue line represents the index contraction, and the large triangle to the left of the blue line represents the state $|X'\rangle_{r'R'}$; after index contraction, the left diagram is simplified to the right figure with an additional coefficient $\frac{1}{|X|}$.

schematic diagram to the index contraction on the region rr' , we need to multiply it by an additional factor of $\frac{1}{|X|}$.

After simplifying the diagram, we can more conveniently describe the calculation process of the n -th Rényi entropy of the radiation, whose density matrix is:

$$\rho_{RR'}(\tilde{U}) = \text{tr}_{BB'} \left(\tilde{V} \otimes I_{RR'} |\psi\rangle\langle\psi| \tilde{V}^\dagger \otimes I_{RR'} \right). \quad (2.12)$$

As shown in Fig. 5, we replicate the system n times, resulting in n pairs of \tilde{U} and \tilde{U}^\dagger . From equation (2.6), for each \tilde{V} or \tilde{V}^\dagger , the normalization factor is $|X|$, so the total normalization factor is $|X|^{2n}$. In Fig. 5 we have n factors of $\frac{1}{|X|}$ from n index contractions, so the whole coefficient should be $|X|^n$. The Haar integral can be expressed as

$$\int d\tilde{U} \prod_{i=1}^n \tilde{U}_{y_i x_i} \tilde{U}_{x_{\tau(i)} y_i}^\dagger = \frac{1}{N^n} \sum_{\sigma \in S_n} \prod_{i=1}^n \delta_{x_i x_{\sigma \tau(i)}} \delta_{y_i y_{\sigma(i)}} = \frac{1}{N^n} \sum_{\sigma \in S_n} |X|^{\|\sigma \circ \tau\|} |Y|^{\|\sigma\|} \quad (2.13)$$

where x and y correspond to the indices of regions rr' and BB' , respectively, i labels the i -th copy; τ and σ belong to the elements of permutation group S_n : τ is the cyclic permutation and σ is any group element; $|\sigma|$ represents the number of cycles in the permutation σ .

We can generally write the expression for the n -th Rényi entropy as

$$S^{(n)} = -\frac{1}{n-1} \log \left(\sum_{\sigma \in S_n} f_n(\sigma) \right). \quad (2.14)$$

When we find the maximum value f_n^{\max} in $f_n(\sigma)$, we have

$$-\frac{1}{n-1} \log(f_n^{\max}) - \frac{1}{n-1} \log(\Gamma(n+1)) \leq S^{(n)} \leq -\frac{1}{n-1} \log(f_n^{\max}). \quad (2.15)$$

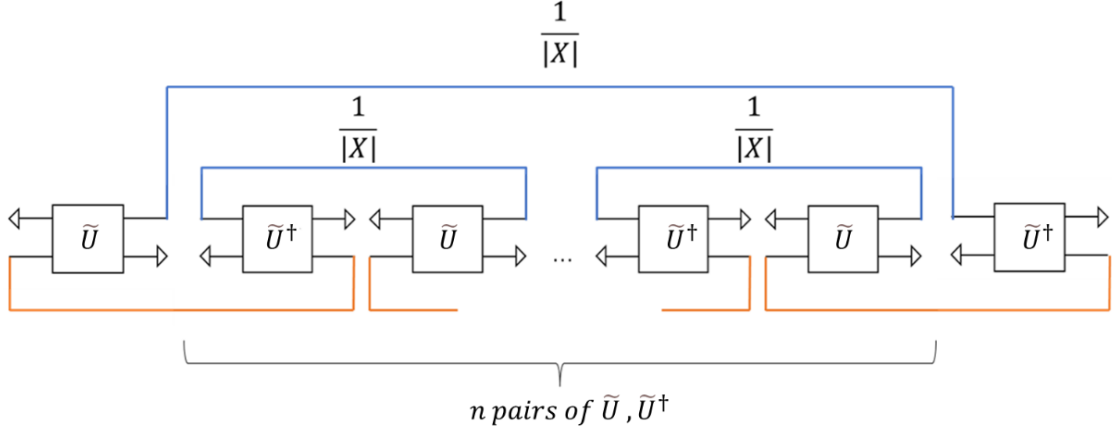


Figure 5. The diagram illustrating the calculation of the n -th Rényi entropy. The red lines represent the contraction of indices over the regions B and B' . After contracting the red lines, we obtain the density matrix of the radiation region, $\rho_{RR'}(\tilde{U})$. The blue lines represent the contraction of indices over the regions R and R' . We replicate the density matrix n times, and the contraction of the blue lines represents the operation of multiplying the n copies of the density matrix and taking the trace, where the indices x of \tilde{U}^\dagger are cyclically permuted.

Fitting as n tends to 1, we see that

$$-\lim_{n \rightarrow 1} \frac{1}{n-1} \log(f_n^{\max}) - (1-\gamma) \leq S^{(1)} \leq -\lim_{n \rightarrow 1} \frac{1}{n-1} \log(f_n^{\max}) \quad (2.16)$$

where $\gamma = 0.577\dots$, i.e.

$$S^{(1)} = -\lim_{n \rightarrow 1} \frac{1}{n-1} \log(f_n^{\max}) + O(1). \quad (2.17)$$

In the summation (2.13), because $|X|$ and $|Y|$ are much larger than 1, we only need to find the dominant contribution.

According to [48], we have $|\sigma| + |\sigma \circ \tau| \leq n + 1$. Thus, when $|X| \geq |Y|$, the term with the largest $|\sigma \circ \tau|$ dominates. In this case, $\sigma = \tau^{-1}$, so $|\sigma \circ \tau| = |e| = n$ and $|\sigma| = |\tau^{-1}| = 1$. Multiplying by the coefficient $|X|^n$, the expression for the Rényi entropy in this case is

$$\int d\tilde{U} \text{tr}(\rho_{RR'}^n(\tilde{U})) = \frac{1}{|Y|^{n-1}}. \quad (2.18)$$

When $|X| \leq |Y|$, the term with the largest $|\sigma|$ dominates. In this case, $\sigma = e$, so $|\sigma \circ \tau| = |\tau| = 1$ and $|\sigma| = |e| = n$, where e is the identity element. Multiplying by the factor $|X|^n$, the expression for the Rényi entropy in this case is

$$\int d\tilde{U} \text{tr}(\rho_{RR'}^n(\tilde{U})) = \frac{1}{|X|^{n-1}}. \quad (2.19)$$

Thus, the fine-grained entropy of the radiation is

$$S(RR') = 2 \min(\log |R|, \log |B|), \quad (2.20)$$

which agrees with the result given by the QES formula.

3 Reflected entropy

In this section, we would like to compute the reflected entropies between different regions in the two-sided black hole model. First, let us review the definition of the reflected entropy [27]. For a subsystem AC , its Hilbert space can be factorized into a direct product of two sub-Hilbert spaces $\mathcal{H}_{AC} = \mathcal{H}_A \otimes \mathcal{H}_C$. The density matrix on AC is ρ_{AC} . It can be canonically purified on a double Hilbert space $\mathcal{H}_A \otimes \mathcal{H}_C \otimes \mathcal{H}_{A^*} \otimes \mathcal{H}_{C^*}$ to $|\sqrt{\rho_{AC}}\rangle$ with

$$|\sqrt{\rho_{AC}}\rangle = \rho_{AC} \otimes I_{A^*C^*} |\phi_{AC}^+\rangle \quad (3.1)$$

where $I_{A^*C^*}$ is the identity matrix and $|\phi_{AC}^+\rangle$ is a maximally entangled state without normalization factor, $\sum_i |i\rangle_{AC} |i\rangle_{A^*C^*}$. The reflected entropy between A and C is defined as

$$S_R(A : C) \equiv S(AA^*)_{\sqrt{\rho_{AC}}} = S(\rho_{AA^*}) \quad (3.2)$$

where $\rho_{AA^*} = \text{tr}_{CC^*}(|\sqrt{\rho_{AC}}\rangle \langle \sqrt{\rho_{AC}}|)$ is the reduced density matrix of the AA^* subsystem.

Based on the strong subadditivity of the entanglement entropy we can determine the upper and lower bounds for the reflected entropy:

$$I(A : C) \leq S_R(A : C) \leq 2 \min(S(A), S(C)). \quad (3.3)$$

In the following, in addition to calculating the reflected entropy, we also calculate the mutual information. Actually, we may define the so-called Markov gap[66],

$$S_R(A : C) - I(A : C), \quad (3.4)$$

which can be related to the fidelity of a particular Markov recovery process on the canonical purification of ρ_{AC} .

As the computation of the entanglement entropy, one may calculate the n -th Rényi reflected entropy first and then do analytical continuation $n \rightarrow 1$ to obtain the reflected entropy. However, unlike the usual entanglement entropy, the calculation of the reflected entropy involves the operator $\sqrt{\rho_{AC}}$, which is not easy to define and compute. To solve this problem, one introduce a new replication on $\sqrt{\rho_{AC}}$ [27] to define a normalized state,

$$|\phi^{(m)}\rangle = \text{tr}(\rho_{AC}^m)^{-1/2} |\rho_{AC}^{m/2}\rangle. \quad (3.5)$$

When m approaches 1, we return to our initially defined purification. When m is even, the terms containing $\sqrt{\rho_{AC}}$ do not appear, making the calculation easy. At the same time, considering n copies for the n -th Rényi entropy, one obtain a (m, n) -th Rényi entropy, and the reflected von Neumann entropy is given by

$$S_R(A : C) = \lim_{m,n \rightarrow 1} \frac{1}{1-n} \log \text{tr} \left(\text{tr}_{CC^*} \left(|\phi^{(m)}\rangle\langle\phi^{(m)}| \right)^n \right). \quad (3.6)$$

In the following calculation, it is necessary to take the average over the Haar measure. To prevent the denominator from containing the unitary matrix random variable, we should first take average on the normalized denominator

$$|\overline{\phi^{(m)}}\rangle = \text{tr} \left(\overline{\rho_{AC}^m} \right)^{-1/2} |\rho_{AC}^{m/2}\rangle. \quad (3.7)$$

The modified definition of reflected entropy is

$$S_R(A : C) = \lim_{m,n \rightarrow 1} \frac{1}{1-n} \log \text{tr} \left(\overline{\text{tr}_{CC^*} \left(|\overline{\phi^{(m)}}\rangle\langle\overline{\phi^{(m)}}| \right)^n} \right). \quad (3.8)$$

In this definition, when averaging over the Haar measure, we can conveniently apply the Haar measure integration formula (2.10).

3.1 Reflective entropy between black holes

In this subsection, our goal is to calculate the reflected entropy $S_R(B : B')$ and the mutual information $I(B : B')$ between the black hole regions on two sides.

First, we calculate the mutual information between the two black hole regions B and B' , given by

$$I(B : B') = S(B) + S(B') - S(BB'). \quad (3.9)$$

Since the entire system in our model is in a pure state, the entanglement entropy of the two-sided black hole region $S(BB')$ should be equal to the one of the two-sided radiation region $S(RR')$. According to (2.20), we obtain

$$S(BB') = 2 \min(\log |R|, \log |B|). \quad (3.10)$$

Due to symmetry, we expect that $S(B)$ is equal to $S(B')$. Therefore, the only quantity we need to calculate is the entanglement entropy corresponding to the region B . The reduced density matrix of B is

$$\rho_B(\tilde{U}) = \text{tr}_{RR'B'} \left(\tilde{V} \otimes I_{RR'} |\psi\rangle\langle\psi| \tilde{V}^\dagger \otimes I_{RR'} \right) \quad (3.11)$$

We can calculate the n -th Rényi entropy of the region B . From Fig. 6, similar to the previous analysis, we can factor out a coefficient $|X|^n$, and for the Haar integral we have

$$\int d\tilde{U} \prod_{i=1}^n \tilde{U}_{B_i B'_i; x_i} \tilde{U}_{x_i; B_{\tau(i)} B'_i}^\dagger = \frac{1}{N^n} \sum_{\sigma \in S_n} \prod_{i=1}^n \delta_{B_i B_{\sigma(\tau(i))}} \delta_{B'_i B'_{\sigma(i)}} \delta_{x_i x_{\sigma(i)}} = \frac{1}{N^n} \sum_{\sigma \in S_n} |B|^{|\sigma \circ \tau| + |\sigma|} |X|^{\sigma}. \quad (3.12)$$

Since $|\sigma \circ \tau| + |\sigma| \leq n + 1$, the equality holds when σ is the identity element, and $|\sigma| = |e| = n$ takes the maximum value. Thus, the n -th Rényi entropy of B satisfies

$$\int dU \text{tr}(\rho_B^n(\tilde{U})) = \frac{1}{|B|^{n-1}}. \quad (3.13)$$

The von Neumann entropy of B is simply

$$S(B) = \log |B|. \quad (3.14)$$

Thus we can obtain an expression for the mutual information based on the above results,

$$I(B : B') = 2 \max(\log |B| - \log |R|, 0). \quad (3.15)$$

Therefore, we see that the quantum correlation between the black holes gets weakened by the Hawking radiations. After the Page time, there is no longer correlation between the two black holes, and all the degrees of freedom in the black holes are entangled with R and R' .

Now we turn to the calculation of the reflected entropy $S_R(B : B')$. For the purification defined in (3.1), its effect on the external legs is merely to rotate the directions of the external legs by 180 degrees (from the perspective of the diagram), meaning that the vector corresponding to the external leg is turned to its dual vector. Because the maximally entangled state $|\phi^+\rangle$ does not have a normalization factor, we do not need to add any additional factors before the expression. Now we consider the m -replicated state $|\phi^{(m)}\rangle$. We can first calculate its denominator $\text{tr}(\overline{\rho_{BB'}^m})^{1/2}$, which after averaging becomes a coefficient outside the Haar integral. To read the m -th Rényi entropy of the two-sided black hole region BB' , we need to compute $\text{tr}(\overline{\rho_{BB'}^m})$ and have

$$\text{tr}(\overline{\rho_{BB'}^m}) = \max \left(\frac{1}{|X|^{m-1}}, \frac{1}{|Y|^{m-1}} \right). \quad (3.16)$$

To compute the reflected entropy, we need to consider the (m, n) -th Rényi entropy by using double-replica trick, which requires us to replicate the density matrix n times, so the denominator, when multiplied n times, contributes a factor of $\left(\max \left(\frac{1}{|X|^{m-1}}, \frac{1}{|Y|^{m-1}} \right) \right)^{-n}$.

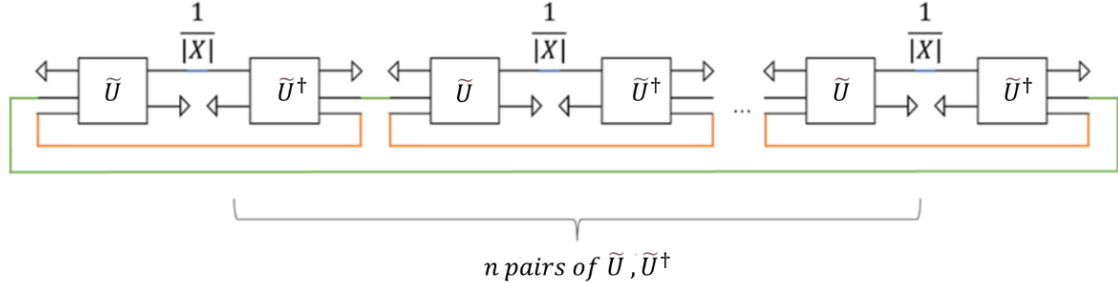


Figure 6. The diagram showing how to compute the n -th power of the reduced density matrix of region B . In this diagram, the blue line represents the simplified index contraction multiplied by a factor of $\frac{1}{|X|}$, the red line represents the index contraction for the region B' , and the green line represents the index contraction and taking trace of the n replicated reduced density matrices of B . Using the indices of \tilde{U} as the basis, among the indices of \tilde{U}^\dagger , the red line corresponds to the B' and the blue line corresponds to the X with the same indices as \tilde{U} , while the green line corresponds to the indices of B with a cyclic permutation of the n elements.

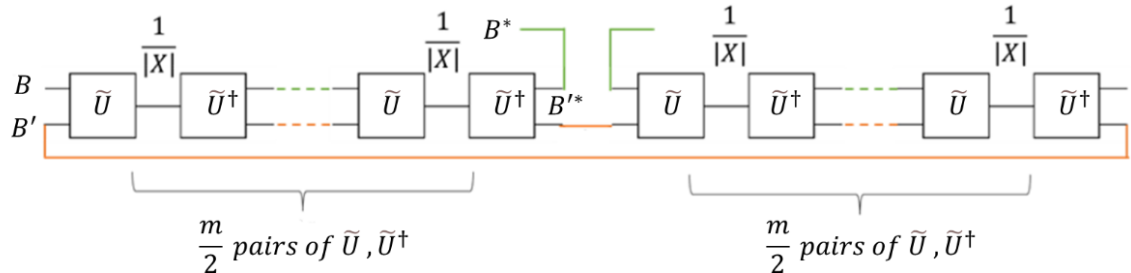


Figure 7. The diagram showing the computation of the numerator of the reduced density matrix $\text{tr}_{B'B'^*}(|\rho_{BB'}^{m/2}\rangle\langle\rho_{BB'}^{m/2}|)$, for even m replicated states. The fixed external legs were omitted as they do not affect the calculation. We have labeled the regions corresponding to each external leg. From the green solid lines, it can be seen that the conjugate transpose of the degrees of freedom corresponding to B becomes the degrees of freedom for B^* .

After handling the coefficient contributed by the denominator, we next need to calculate the numerator of the reduced density matrix $\text{tr}_{B'B'^*}(|\rho_{BB'}^{m/2}\rangle\langle\rho_{BB'}^{m/2}|)$. We refer to the copied region for the two-sided black hole region BB' as $B^*B'^*$. Actually, to compute the reflected Rényi entropy, m should be even. In this case, we can use the diagram shown in Fig. 7. We have a total of m pairs of \tilde{U} and \tilde{U}^\dagger such that the reduced density matrix corresponding to $|\phi^{(m)}\rangle$ gives rise to a factor of $\frac{1}{|X|^m}$. Taking into account the fact that computing the (m, n) -th Rényi entropy requires replicating n

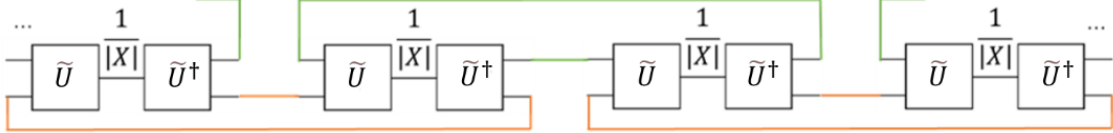


Figure 8. When $m = 2$, the diagram for the numerator of the reduced density matrix. The red lines and green lines represent the index contractions in regions B' and B respectively, while the black lines represent the index contractions in x , accompanied by a factor of $\frac{1}{|X|}$. From the cyclic units, it is easy to see that if the indices of \tilde{U} are fixed, the indices x of \tilde{U}^\dagger correspond one-to-one with the indices x of \tilde{U} . The indices B and B' of \tilde{U}^\dagger are composed of a series of length m cycles, arranged in an interleaved manner. The end of one cycle of one index is located in the middle of the cycle of the other index. From this, the expressions for g_1 and g_2 can be read.

times, we find a factor of $\frac{1}{|X|^{mn}}$. Meanwhile, the normalization factor for nm pairs of \tilde{U} and \tilde{U}^\dagger is $|X|^{2mn}$. Therefore, before calculating the Haar integral, we should multiply it by an overall coefficient

$$|X|^{mn} \left(\max \left(\frac{1}{|X|^{m-1}}, \frac{1}{|Y|^{m-1}} \right) \right)^{-n} \quad (3.17)$$

The relevant Haar integral is

$$\int d\tilde{U} \prod_{i=1}^{nm} \tilde{U}_{B_i B'_i; x_i} \tilde{U}_{x_i; B_{g_2(i)} B'_{g_1(i)}} = \frac{1}{N^{mn}} \sum_{\sigma \in S_n} |B|^{|\sigma \circ g_1| + |\sigma \circ g_2|} |X|^{|\sigma|}, \quad (3.18)$$

where g_1 and g_2 are two group elements in the permutation group S_n , satisfying

$$g_1 = (1, 2, \dots, m) \dots (n-m+1, \dots, n), \quad (3.19)$$

$$g_2 = \left(\frac{m}{2} + 1, \dots, \frac{3m}{2} \right) \dots \left(\left(n - \frac{1}{2} \right) m + 1, \dots, nm, 1, \dots, \frac{m}{2} \right). \quad (3.20)$$

We show the calculation of $(2, n)$ -th reflected Rényi entropy in Fig. 8.

When $|X| \geq |Y|$, namely the dimension of the radiation region is larger than that of the black hole region, corresponding to the late evaporation stage, the dominant term in (3.18) is the one that $|\sigma|$ takes the maximum value. In this case, σ must be the identity element e with $|\sigma| = nm$, and $|\sigma \circ g_1| + |\sigma \circ g_2| = 2n$. Thus, multiplying by the factor $|X|^{mn}|Y|^{mn-n}$, we obtain the reflected entropy:

$$S_R(B : B') = 0. \quad (3.21)$$

This indicates that in the late evaporation stage, the reflected entropy $S_R(B : B')$ reaches its lower bound, simply vanishing.

When $|X| \leq |Y|$, namely the dimension of the radiation region is smaller than that of the black hole region, corresponding to the early evaporation stage, the situation is more complex. We need to introduce the Cayley distance[48], defined by the minimal number of transpositions. For the permutation group S_n , let α, β be group elements, then we have the Cayley distance

$$d(\alpha, \beta) = n - |\alpha \circ \beta^{-1}|. \quad (3.22)$$

The Cayley distance satisfies the triangle inequality,

$$d(\alpha, \beta) + d(\beta, \gamma) \geq d(\alpha, \gamma). \quad (3.23)$$

Thus, we obtain

$$|\sigma \circ g_1| + |\sigma \circ g_2| \leq 2nm - 2n + 2. \quad (3.24)$$

If $|Y|$ is large enough, we need to first consider the exponent of $|Y|$. In order to get the dominant term in (3.18), we need the inequality to be saturated. In terms of the Cayley distance this requires that the σ should be a permutation of the minimal number of transposition from g_1 to g_2 :

$$d(g_1, \sigma^{-1}) + d(\sigma^{-1}, g_2) = d(g_1, g_2). \quad (3.25)$$

We find that g_1 and g_2 differ by integer multiples of $m/2$, from 1 to nm . As $g_1^{-1}g_2$ is the transposition from g_1 to g_2 , if we omit the identical maps, $g_1^{-1}g_2$ can be written as

$$g_1^{-1}g_2 = \left(m, \frac{m}{2}, 2m, \frac{3m}{2}, \dots, nm, (n - \frac{1}{2})m \atop nm, \frac{3m}{2}, m, \frac{5m}{2}, \dots, (n - 1)m, \frac{m}{2} \right). \quad (3.26)$$

In this case, σ^{-1} belongs to one of the minimal number of transpositions, namely σ^{-1} is in an intermediate process of the cycle of $(m, 2m, \dots, nm)$ and $(m/2, 3m/2, (n-1/2)m)$. Then we need to choose a σ with maximal $|\sigma|$ in these intermediate processes. By induction we find that when $\sigma = g_1^{-1}$ or $\sigma = g_2^{-1}$, $|\sigma|$ has a maximum value n . Thus, multiplying by the factor $|X|^{2mn-n}$, we obtain the reflected entropy:

$$S_R(B : B') = 2 \log |B|. \quad (3.27)$$

But if $\log |X|$ and $\log |Y|$ are comparable, when the exponent $\frac{1}{2}(|\sigma \circ g_1| + |\sigma \circ g_2|)$ of $|Y|$ decreases and the exponent $|\sigma|$ of $|X|$ increases, $|B|^{|\sigma \circ g_1| + |\sigma \circ g_2|} |X|^{|\sigma|}$ may increase.

Considering $\frac{1}{2}(|\sigma \circ g_1| + |\sigma \circ g_2|) + |\sigma| \leq nm + 2n$, when $\frac{1}{2}(|\sigma \circ g_1| + |\sigma \circ g_2|)$ decreases by 1 from its maximum value, $|\sigma|$ can increase by at most n , which happens when

$$\sigma = (1, 2, \dots, \frac{m}{2})^{-1} (\frac{m}{2} + 1, \frac{m}{2} + 2, \dots, m)^{-1} \dots ((n - \frac{1}{2})m + 1, \dots, nm)^{-1}. \quad (3.28)$$

So strictly speaking, the derivation to (3.27) is valid only when $|X|^n \leq |Y|$. However, if we take $n \rightarrow 1$, this requirement goes back to $|X| \leq |Y|$. In the following computations, we will use the same treatment.

Considering the upper bound of the reflected entropy

$$2 \min(S(B), S(B')) = 2 \log |B|, \quad (3.29)$$

we see that when the dimension of the radiation region is smaller than that of the black hole region (early evaporation), the reflected entropy $S_R(B : B')$ equals its upper bound $2 \log |B|$. On the contrary, when the dimension of the radiation region is larger than that of the black hole region (late evaporation), the reflected entropy $S_R(B : B')$ equals its lower bound, 0.

In the late stage of evaporation, the fact that the entanglement entropy of the radiation region equals the black hole entropy $2 \log |B|$ suggests that at this time, the black hole region and the radiation region are maximally entangled, and there is no entanglement between the two black hole regions. Hence, the reflected entropy is zero. This picture has also been verified in the two-sided black hole model in which the JT gravity is coupled with a conformal field theory[31]. In fact, if we take the high-temperature limit $\beta \rightarrow 0$, the reflected entropy Eq. (5.19) in [31]

$$S_R(B_L : B_R) = 2S_0 + 2\Phi_r + \frac{c}{3}(b - \ln \cosh t + \ln 2) \quad (3.30)$$

can be approximated as

$$S_R(B_L : B_R) = \frac{2\pi c}{3\beta}(b - t). \quad (3.31)$$

The single-side black hole entropy Eq.(D.1) in [31]

$$S(B_L) = S_0 + \frac{\phi_r}{\tanh d} + \frac{c}{6} \ln \frac{4 \sinh^2 \frac{b+d}{2}}{\sinh d} \quad (3.32)$$

can be approximated as

$$S(B_L) = \frac{\pi c}{3\beta}b. \quad (3.33)$$

So before the evaporation the reflected entropy between the two black holes in the JT gravity+CFT model $S_R(B_L : B_R)$ also equals the upper bound $2S(B_L)$.

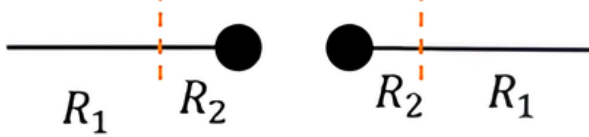


Figure 9. For the partition of the two-sided radiation region, the red dashed line divides the radiation region on one side into two sub-regions R_1 and R_2 . Both of these two sub-regions are disconnected but are symmetrically distributed in the radiation region R and its copy. In our model, due to the symmetry of the unitary matrix \tilde{U} , other less symmetric partitions might yield the same result.

In the early stage of evaporation, although there is an entanglement entropy $2 \log |R|$ in the radiation region, the dimension of the black hole region is larger than that of the radiation region. Therefore, the two black holes are approximately in a pure state, and the reflected entropy is saturated at the upper bound $2 \log |B|$. It is worth noting that in our model, the contribution of the entanglement between the black hole region and the radiation region to the reflected entropy is of higher order. This also leads to a discontinuous transition of the reflected entropy at the Page time, while the transition of the Page curve of the entanglement entropy only has a discontinuity in the first derivative at the Page time.

3.2 Reflective entropy between radiations

Here we are not going to study the reflected entropy between the radiations on two sides. Instead, we partition the whole radiation region in a way similar to that employed in [31]. Specifically, we cut the radiation region and its copy at the same positions to obtain two regions R_1 and R_2 , as shown in Fig. 9. Note that both sub-regions R_1 and R_2 are disconnected and distributed in a symmetric way.

Similar to the previous subsection, we first compute the mutual information $I(R_1 : R_2)$, assuming without loss of generality that $|R_1| > |R_2|$. In the mutual information

$$I(R_1 : R_2) = S(R_1) + S(R_2) - S(R_1 R_2), \quad (3.34)$$

$S(R_1 R_2)$ is the von Neumann entropy of the whole radiation region R , given by

$$S(R_1 R_2) = 2 \min(\log |R|, \log |B|). \quad (3.35)$$

Next, we need to compute $S(R_1)$ and $S(R_2)$. Similar to the previous calculation of Rényi entropy, the key lies in identifying the index correspondence in the Haar integral and determining the dominant elements in the permutation group S_n . Analogous to the

previous calculations, the coefficient is $|X|^n$, and the expression for the Haar integral is

$$\int d\tilde{U} \prod_{i=1}^{nm} \tilde{U}_{y_i; R_{1i} R_{2i}} \tilde{U}_{R_{1\tau(i)} R_{2i}; y_i} = \frac{1}{N^n} \sum_{\sigma \in S_n} |Y|^{\sigma|} |R_2|^{\sigma|} |R_1|^{\sigma \circ \tau|}. \quad (3.36)$$

When $|R_1| \geq |R_2| |Y|$, σ should be taken as the inverse of an n -cycle permutation τ^{-1} such that $|\sigma \circ \tau| = n$. As $|\sigma| = 1$, and multiplying by $|X|^n$, we find the n -th Rényi entropy and further obtain the von Neumann entropy of the region R_1 ,

$$S(R_1) = 2 \log |B| + \log |R_2|. \quad (3.37)$$

When $|R_1| \leq |R_2| |Y|$, σ should be the identity element e , $|\sigma \circ \tau| = 1$, $|\sigma| = n$, and multiplying by $|X|^n$ gives the n -th Rényi entropy. Then, we obtain the von Neumann entropy of the region R_1 ,

$$S(R_1) = \log |R_1|. \quad (3.38)$$

From the above discussion, we have

$$S(R_1) = \min(\log |R_1|, 2 \log |B| + \log |R_2|). \quad (3.39)$$

Symmetrically, we obtain the expression for the von Neumann entropy of region R_2 :

$$S(R_2) = \min(\log |R_2|, 2 \log |B| + \log |R_1|) = \log |R_2|. \quad (3.40)$$

Finally, we have the mutual information $I(R_1 : R_2)$ between the regions R_1 and R_2 with $|R_1| > |R_2|$

$$I(R_1 : R_2) = S(R_1) + \log |R_2| - 2 \min(\log |R_1|, \log |B|) \quad (3.41)$$

It can be classified into three stages, with two transition points. The first transition occurs at $|R| = |B|$, which corresponds to the Page time. The second transition occurs at $|R_1| = |B|^2 |R_2|$, which was called the Page time for the region R_1 [31]. Before the first transition, the mutual information $I(R_1 : R_2) = 0$; between the first and second transitions, $I(R_1 : R_2) = 2 \log |R| - 2 \log |B|$; and after the second transition, $I(R_1 : R_2) = 2 \log |R_2|$. In summary, we have ($|R_1| > |R_2|$)

$$I(R_1 : R_2) = \begin{cases} 0, & \text{when } |R_1| |R_2| \leq |B| \\ 2 \log |R| - 2 \log |B|, & \text{when } |B| |R_2|^{-1} \leq |R_1| \leq |B|^2 |R_2| \\ 2 \log |R_2|, & \text{when } |R_1| \geq |B|^2 |R_2|. \end{cases} \quad (3.42)$$

This three-stage behavior in the mutual information also appears in Fig. 5.7 of [31].

Next, we consider the reflected entropy between the region R_1 and the region R_2 . Similar to the previous calculations, we first compute the denominator. Since the total

system is in a pure state, the value of the denominator is the same as in the previous section. We then obtain the Haar integral multiplied by the coefficient (considering (m, n) -th Rényi entropy)

$$|X|^{mn} \left(\max \left(\frac{1}{|X|^{m-1}}, \frac{1}{|Y|^{m-1}} \right) \right)^{-n}. \quad (3.43)$$

Next, we identify the elements of the permutation group S_n corresponding to the ways in contracting the nm replicated external legs. Due to the asymmetry between the region R_1 and the region R_2 , the Haar integral corresponding to the (m, n) -th Rényi reflected entropy between the regions R_1 and R_2 differs slightly from the Haar integral corresponding to the (m, n) -th Rényi reflected entropy of the black holes BB' . Finally, we read

$$\int d\tilde{U} \prod_{i=1}^{nm} \tilde{U}_{y_i; R_{1i} R_{2i}} \tilde{U}_{R_{1g_2(i)} R_{2g_1(i)}; y_i}^\dagger = \frac{1}{N^{mn}} \sum_{\sigma \in S_n} |R_1|^{|\sigma \circ g_2|} |R_2|^{|\sigma \circ g_1|} |Y|^{|\sigma|}. \quad (3.44)$$

When $|Y| \geq |X|$, σ should be taken as the identity element. The dominant term is $|R_1|^n |R_2|^n |Y|^{nm} = |X|^n |Y|^{nm}$, resulting in the (m, n) -th Rényi entropy being zero. Thus, we obtain the reflected entropy between the region R_1 and the region R_2 :

$$S_R(R_1 : R_2) = 0. \quad (3.45)$$

When $|Y| \leq |X|$, given $|R_1| > |R_2|$, σ should be taken as the inverse of g_2 to ensure the exponent of $|R_1|$ reaches its maximum. The dominant term is $|R_1|^{nm} |R_2|^{nm-2n+2} |Y|^{nm} = |X|^{nm} |Y|^n |R_2|^{-2n+2}$. We obtain the reflected entropy between the region R_1 and the region R_2 :

$$S_R(R_1 : R_2) = 2 \log |R_2|. \quad (3.46)$$

Meanwhile, we can compute the upper bound of the reflected entropy $S_R(R_1 : R_2)$:

$$2 \min(S(R_1), S(R_2)) = 2S(R_2) = 2 \log |R_2|. \quad (3.47)$$

Based on the above results, we find that before the Page time, the reflected entropy $S_R(R_1 : R_2)$ is at its lower bound, and after the Page time, the reflected entropy $S_R(R_1 : R_2)$ is at its upper bound. In short, we have

$$S_R(R_1 : R_2) = \begin{cases} 0, & \text{when } |R_1||R_2| \leq |B| \\ 2 \min(\log |R_1|, \log |R_2|), & \text{when } |R_1||R_2| > |B|. \end{cases} \quad (3.48)$$

The result here is the same as the one in [35], where the reflected entropy in West Coast model was studied.

There is only one transition for the reflected entropy between the region R_1 and the region R_2 , and no transition at the Page time for R_1 . Additionally, under the partition of the regions R_1 and R_2 , the transition of the reflected entropy $S_R(R_1 : R_2)$ is discontinuous, whereas the two transitions of the mutual information $I(R_1 : R_2)$ are continuous.

3.3 Radiation and black hole

For an evaporating single-sided black hole, its fundamental description involves the entanglement between a boundary quantum system B and a single-sided radiation system R . In the case of a two-sided black hole coupled with a two-sided radiation system, the fundamental description is composed of the region of the original single-sided black hole BR and its mirror copy $B'R'$ so that the whole system gets canonically purified. This purification process conforms to the definition of reflected entropy, thus we should have

$$S_R^{(s)}(R : B) = S(RR'). \quad (3.49)$$

The reflected entropy $S_R^{(s)}(R : B)$ between the radiation subregion R and the black hole subregion B in the single-sided evaporating black hole system, should be equal to the entanglement entropy of the two-sided radiation region RR' in the two-sided evaporating black hole system.

However, it is worth noting that in our model, the purification is defined in the effective description, while the entropy calculation is performed by using the non-isometric mapping in the fundamental description. There is no direct quantitative relationship between the holographic mapping corresponding to the single-sided black hole and the one corresponding to the two-sided black hole, i.e., $\tilde{V} \neq V \otimes V$, but we can verify that for the holographic mapping described in this work, the relationship in equation (3.49) still holds.

In order to calculate the reflected entropy $S_R^{(s)}(R : B)$ between the radiation subregion R and the black hole subregion B in the single-sided evaporating black hole model, we first consider the properties of the reduced density matrix corresponding to a single radiation region R , as shown in Fig. 10, where U and U^\dagger are defined by (2.4). By simplifying the maximally entangled state to the external leg representing the dual vector, the normalization factor of the two maximally entangled states provides a factor of $\frac{1}{|R|}$. After knowing the form of the reduced density matrix, we are able to calculate the (m, n) -th Rényi entropy. For the denominator, we have[23]

$$\text{tr}(\overline{\rho_{BR}^m}) = \max \left(\frac{1}{|R|^{m-1}}, \frac{\text{tr}(\rho_s^m)}{|B|^{m-1}} \right). \quad (3.50)$$

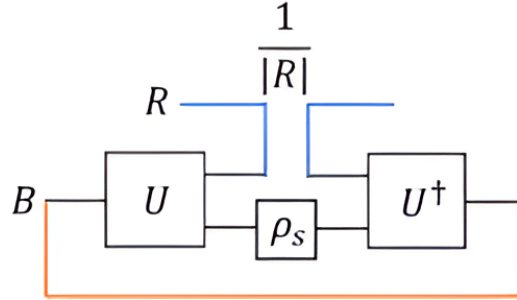


Figure 10. The diagram of the reduced density matrix corresponding to the radiation region in the single-sided evaporating black hole model. The three indices B , R , and s that need to be summed are all marked in the figure. The red lines represent the tracing out of the single-sided black hole region when calculating the reduced density matrix. The blue curves represent the contraction of the unitary matrices U and U^\dagger with the maximally entangled states on r and R .

Combined with the previous discussion, a pair of U and U^\dagger corresponds to a coefficient of $\frac{1}{|R|}$, and from (2.4), the normalization coefficient for a pair of U and U^\dagger is $|R|^2$. As a result, we get the total coefficient

$$|R|^{mn} \max \left(\frac{1}{|R|^{m-1}}, \frac{\text{tr}(\rho_s^m)}{|B|^{m-1}} \right)^{-n}. \quad (3.51)$$

We can also calculate the form of the Haar measure integration as

$$\int dU \prod_{i=1}^{nm} U_{B_i; R_i a_i} \rho_{s a_i b_i} U_{R_{g_2(i)} b_i; B_{g_1(i)}}^\dagger = \frac{1}{N^{mn}} \sum_{\sigma \in S_n} (|R|^{\|\sigma \circ g_2\|} |B|^{\|\sigma \circ g_1\|} \prod_{r=1}^{|\sigma|} \text{tr}(\rho_s^{c_r(\sigma)})), \quad (3.52)$$

where a, b are the indices of ρ_s , and c_r is the length of the r -th cycle in the group element σ , satisfying $\sum_{r=1}^{|\sigma|} c_r(\sigma) = n$. According to the properties of the density matrix, the dominant term is obtained when $\sigma = g_1^{-1}$ or $\sigma = g_2^{-1}$. When $|R| \leq |B|$, the dominant contribution is $|R|^{nm-2n+2} |B|^{nm} \text{tr}(\rho_s^m)^n$. In this case, the reflected von Neumann entropy is

$$S_R^{(s)}(R : B) = 2 \log |R|. \quad (3.53)$$

When $|R| \geq |B|$, the dominant contribution is $|R|^{nm} |B|^{nm-2n+2} \text{tr}(\rho_s^m)^n$ and the reflected von Neumann entropy is

$$S_R^{(s)}(R : B) = 2 \log |B|. \quad (3.54)$$

Thus we have

$$S_R^{(s)}(R : B) = 2 \min(\log |R|, \log |B|) = S(RR'). \quad (3.55)$$

That is, in the single-sided evaporating black hole model, the reflected entropy $S_R^{(s)}(R : B)$ between the radiation subregion R and the black hole subregion B is equal to the entanglement entropy $S(RR')$ of the two-sided radiation in the two-sided evaporating black hole model.

Going a step further, if we purify multiple small single-sided black holes and perform the replacement $V \otimes V \rightarrow \tilde{V}$ multiple times, we can study the case of multi-sided black holes. By applying the previous computational techniques, we can study the multi-entropy and reflected entropy on evaporating multi-sided black holes. (Some previous studies can be found in[28, 47, 71].)

4 Conclusion and discussion

In this paper, we introduced a two-sided evaporating black hole model by using a post-selection map defined by a Haar random unitary matrix. We investigated the entanglement entropy and reflected entropy in this model through a non-isometric map. The entropy of radiation in the model matches the result from the quantum extremal surface formula and agrees with the Page curve.

In this model, we are allowed to discuss the reflected entropy and the related mutual information between different regions, including the black holes on different sides, the radiations distributed in a symmetric but disconnected way, and the black hole and radiation on single side. The main results are as follows.

- For the reflected entropy between the black holes, it is at its upper bound before the Page time and at its lower bound (zero) after the Page time. The transition at the critical point is discontinuous, similar to the results in [31].
- For the reflected entropy between the radiations, it is at its lower bound before the Page time and at its upper bound after the Page time, coincides with the Page curve of reflected entropy proposed in [35]. The transition at the critical point is discontinuous. In contrast, the corresponding mutual information present a three-stage behavior, undergoing the continuous transitions at the Page time and at the Page time for the region R_1 .
- Finally, we verified that in the single-sided evaporating black hole model, the reflected entropy $S_R(R : B)$ between the radiation subregion R and the black hole subregion B is equal to the entanglement entropy $S(RR')$ of the two-sided evaporating black hole model's radiation.

Our investigations rely on the non-isometric maps from the effective description to fundamental description. Even though the results in this work are consistent with the

ones in other models[31, 35], our method is different from the ones in [30, 31, 35], which based on the semi-classical effective description. It would be interesting to study the reflected entanglement spectrum more carefully and investigate the possible correction to the above picture. Furthermore, our model can also be extended to the case of multi-sided black holes. In future work, we may be able to use our method to explore the multipartite generalization of reflected entropy from a different perspective.

Acknowledgments

We are grateful to Zezhou Hu for useful discussions. This research is supported in part by NSFC Grant No. 11735001, 12275004.

References

- [1] J. M. Maldacena, *The Large N limit of superconformal field theories and supergravity*, *Adv. Theor. Math. Phys.* **2** (1998) 231–252, [[hep-th/9711200](#)].
- [2] D. N. Page, *Information in black hole radiation*, *Phys. Rev. Lett.* **71** (1993) 3743–3746, [[hep-th/9306083](#)].
- [3] D. N. Page, *Time Dependence of Hawking Radiation Entropy*, *JCAP* **09** (2013) 028, [[arXiv:1301.4995](#)].
- [4] N. Engelhardt and A. C. Wall, *Quantum Extremal Surfaces: Holographic Entanglement Entropy beyond the Classical Regime*, *JHEP* **01** (2015) 073, [[arXiv:1408.3203](#)].
- [5] G. Penington, *Entanglement Wedge Reconstruction and the Information Paradox*, *JHEP* **09** (2020) 002, [[arXiv:1905.08255](#)].
- [6] A. Almheiri, N. Engelhardt, D. Marolf, and H. Maxfield, *The entropy of bulk quantum fields and the entanglement wedge of an evaporating black hole*, *JHEP* **12** (2019) 063, [[arXiv:1905.08762](#)].
- [7] A. Almheiri, R. Mahajan, J. Maldacena, and Y. Zhao, *The Page curve of Hawking radiation from semiclassical geometry*, *JHEP* **03** (2020) 149, [[arXiv:1908.10996](#)].
- [8] A. Almheiri, R. Mahajan, and J. Maldacena, *Islands outside the horizon*, [arXiv:1910.11077](#).
- [9] G. Penington, S. H. Shenker, D. Stanford, and Z. Yang, *Replica wormholes and the black hole interior*, *JHEP* **03** (2022) 205, [[arXiv:1911.11977](#)].

[10] A. Almheiri, T. Hartman, J. Maldacena, E. Shaghoulian, and A. Tajdini, *Replica Wormholes and the Entropy of Hawking Radiation*, *JHEP* **05** (2020) 013, [[arXiv:1911.12333](https://arxiv.org/abs/1911.12333)].

[11] H. Geng, *Replica wormholes and entanglement islands in the Karch-Randall braneworld*, *JHEP* **01** (2025) 063, [[arXiv:2405.14872](https://arxiv.org/abs/2405.14872)].

[12] T. Banks, M. R. Douglas, G. T. Horowitz, and E. J. Martinec, *AdS dynamics from conformal field theory*, [hep-th/9808016](https://arxiv.org/abs/hep-th/9808016).

[13] A. Hamilton, D. N. Kabat, G. Lifschytz, and D. A. Lowe, *Holographic representation of local bulk operators*, *Phys. Rev. D* **74** (2006) 066009, [[hep-th/0606141](https://arxiv.org/abs/hep-th/0606141)].

[14] I. Heemskerk, D. Marolf, J. Polchinski, and J. Sully, *Bulk and Transhorizon Measurements in AdS/CFT*, *JHEP* **10** (2012) 165, [[arXiv:1201.3664](https://arxiv.org/abs/1201.3664)].

[15] R. Bousso, B. Freivogel, S. Leichenauer, V. Rosenhaus, and C. Zukowski, *Null Geodesics, Local CFT Operators and AdS/CFT for Subregions*, *Phys. Rev. D* **88** (2013) 064057, [[arXiv:1209.4641](https://arxiv.org/abs/1209.4641)].

[16] B. Czech, J. L. Karczmarek, F. Nogueira, and M. Van Raamsdonk, *The Gravity Dual of a Density Matrix*, *Class. Quant. Grav.* **29** (2012) 155009, [[arXiv:1204.1330](https://arxiv.org/abs/1204.1330)].

[17] A. C. Wall, *Maximin Surfaces, and the Strong Subadditivity of the Covariant Holographic Entanglement Entropy*, *Class. Quant. Grav.* **31** (2014), no. 22 225007, [[arXiv:1211.3494](https://arxiv.org/abs/1211.3494)].

[18] M. Headrick, V. E. Hubeny, A. Lawrence, and M. Rangamani, *Causality & holographic entanglement entropy*, *JHEP* **12** (2014) 162, [[arXiv:1408.6300](https://arxiv.org/abs/1408.6300)].

[19] A. Almheiri, X. Dong, and D. Harlow, *Bulk Locality and Quantum Error Correction in AdS/CFT*, *JHEP* **04** (2015) 163, [[arXiv:1411.7041](https://arxiv.org/abs/1411.7041)].

[20] F. Pastawski, B. Yoshida, D. Harlow, and J. Preskill, *Holographic quantum error-correcting codes: Toy models for the bulk/boundary correspondence*, *JHEP* **06** (2015) 149, [[arXiv:1503.06237](https://arxiv.org/abs/1503.06237)].

[21] X. Dong, D. Harlow, and A. C. Wall, *Reconstruction of Bulk Operators within the Entanglement Wedge in Gauge-Gravity Duality*, *Phys. Rev. Lett.* **117** (2016), no. 2 021601, [[arXiv:1601.05416](https://arxiv.org/abs/1601.05416)].

[22] D. Harlow, *The Ryu-Takayanagi Formula from Quantum Error Correction*, *Commun. Math. Phys.* **354** (2017), no. 3 865–912, [[arXiv:1607.03901](https://arxiv.org/abs/1607.03901)].

[23] C. Akers, N. Engelhardt, D. Harlow, G. Penington, and S. Vardhan, *The black hole interior from non-isometric codes and complexity*, *JHEP* **06** (2024) 155, [[arXiv:2207.06536](https://arxiv.org/abs/2207.06536)].

[24] Z. Gyongyosi, T. J. Hollowood, S. P. Kumar, A. Legramandi, and N. Talwar, *The*

holographic map of an evaporating black hole, JHEP **07** (2023) 043, [[arXiv:2301.08362](https://arxiv.org/abs/2301.08362)].

[25] J. M. Maldacena, *Eternal black holes in anti-de Sitter, JHEP* **04** (2003) 021, [[hep-th/0106112](https://arxiv.org/abs/hep-th/0106112)].

[26] S. D. Mathur, *What is the dual of two entangled CFTs?, arXiv:1402.6378*.

[27] S. Dutta and T. Faulkner, *A canonical purification for the entanglement wedge cross-section, JHEP* **03** (2021) 178, [[arXiv:1905.00577](https://arxiv.org/abs/1905.00577)].

[28] N. Bao and N. Cheng, *Multipartite Reflected Entropy, JHEP* **10** (2019) 102, [[arXiv:1909.03154](https://arxiv.org/abs/1909.03154)].

[29] H.-S. Jeong, K.-Y. Kim, and M. Nishida, *Reflected Entropy and Entanglement Wedge Cross Section with the First Order Correction, JHEP* **12** (2019) 170, [[arXiv:1909.02806](https://arxiv.org/abs/1909.02806)].

[30] V. Chandrasekaran, M. Miyaji, and P. Rath, *Including contributions from entanglement islands to the reflected entropy, Phys. Rev. D* **102** (2020), no. 8 086009, [[arXiv:2006.10754](https://arxiv.org/abs/2006.10754)].

[31] T. Li, J. Chu, and Y. Zhou, *Reflected Entropy for an Evaporating Black Hole, JHEP* **11** (2020) 155, [[arXiv:2006.10846](https://arxiv.org/abs/2006.10846)].

[32] D. Basu, A. Chandra, V. Raj, and G. Sengupta, *Entanglement wedge in flat holography and entanglement negativity, SciPost Phys. Core* **5** (2022) 013, [[arXiv:2106.14896](https://arxiv.org/abs/2106.14896)].

[33] T. Li, M.-K. Yuan, and Y. Zhou, *Defect extremal surface for reflected entropy, JHEP* **01** (2022) 018, [[arXiv:2108.08544](https://arxiv.org/abs/2108.08544)].

[34] Y. Ling, P. Liu, Y. Liu, C. Niu, Z.-Y. Xian, and C.-Y. Zhang, *Reflected entropy in double holography, JHEP* **02** (2022) 037, [[arXiv:2109.09243](https://arxiv.org/abs/2109.09243)].

[35] C. Akers, T. Faulkner, S. Lin, and P. Rath, *The Page curve for reflected entropy, JHEP* **06** (2022) 089, [[arXiv:2201.11730](https://arxiv.org/abs/2201.11730)].

[36] D. Basu, H. Parihar, V. Raj, and G. Sengupta, *Entanglement negativity, reflected entropy, and anomalous gravitation, Phys. Rev. D* **105** (2022), no. 8 086013, [[arXiv:2202.00683](https://arxiv.org/abs/2202.00683)]. [Erratum: Phys.Rev.D 105, 129902 (2022)].

[37] J. K. Basak, H. Chourasiya, V. Raj, and G. Sengupta, *Reflected entropy in Galilean conformal field theories and flat holography, Eur. Phys. J. C* **82** (2022), no. 12 1169, [[arXiv:2202.01201](https://arxiv.org/abs/2202.01201)].

[38] B. Chen, Y. Liu, and B. Yu, *Reflected entropy in $AdS_3/WCFT$, JHEP* **12** (2022) 008, [[arXiv:2205.05582](https://arxiv.org/abs/2205.05582)].

[39] M. J. Vasli, M. R. Mohammadi Mozaffar, K. Babaei Velni, and M. Sahraei,

Holographic study of reflected entropy in anisotropic theories, *Phys. Rev. D* **107** (2023), no. 2 026012, [[arXiv:2207.14169](https://arxiv.org/abs/2207.14169)].

- [40] Y. Lu and J. Lin, *The Markov gap in the presence of islands*, *JHEP* **03** (2023) 043, [[arXiv:2211.06886](https://arxiv.org/abs/2211.06886)].
- [41] M. Afrasiar, J. K. Basak, A. Chandra, and G. Sengupta, *Reflected entropy for communicating black holes. Part I. Karch-Randall braneworlds*, *JHEP* **02** (2023) 203, [[arXiv:2211.13246](https://arxiv.org/abs/2211.13246)].
- [42] M. Afrasiar, J. K. Basak, A. Chandra, and G. Sengupta, *Reflected Entropy for Communicating Black Holes II: Planck Braneworlds*, [arXiv:2302.12810](https://arxiv.org/abs/2302.12810).
- [43] D. Basu, H. Chourasiya, V. Raj, and G. Sengupta, *Reflected entropy in a BCFT on a black hole background*, *JHEP* **05** (2024) 054, [[arXiv:2311.17023](https://arxiv.org/abs/2311.17023)].
- [44] J. K. Basak, D. Basu, V. Malvimat, H. Parihar, and G. Sengupta, *Holographic reflected entropy and islands in interface CFTs*, *JHEP* **05** (2024) 143, [[arXiv:2312.12512](https://arxiv.org/abs/2312.12512)].
- [45] D. Basu and V. Raj, *Reflected entropy and timelike entanglement in TT^- -deformed CFT2s*, *Phys. Rev. D* **110** (2024), no. 4 046009, [[arXiv:2402.07253](https://arxiv.org/abs/2402.07253)].
- [46] B. Ahn, S.-E. Bak, K.-Y. Kim, and M. Nishida, *Renyi reflected entropy and entanglement wedge cross section with cosmic branes in $AdS/BCFT$* , [arXiv:2408.14034](https://arxiv.org/abs/2408.14034).
- [47] M.-K. Yuan, M. Li, and Y. Zhou, *Reflected multi-entropy and its holographic dual*, [arXiv:2410.08546](https://arxiv.org/abs/2410.08546).
- [48] C. Akers, T. Faulkner, S. Lin, and P. Rath, *Reflected entropy in random tensor networks*, *JHEP* **05** (2022) 162, [[arXiv:2112.09122](https://arxiv.org/abs/2112.09122)].
- [49] C. Akers, T. Faulkner, S. Lin, and P. Rath, *Reflected entropy in random tensor networks. Part II. A topological index from canonical purification*, *JHEP* **01** (2023) 067, [[arXiv:2210.15006](https://arxiv.org/abs/2210.15006)].
- [50] B. Czech, S. Shuai, and H. Tang, *Entropies and reflected entropies in the Hayden-Preskill protocol*, *JHEP* **02** (2024) 040, [[arXiv:2310.16988](https://arxiv.org/abs/2310.16988)].
- [51] C. Akers, T. Faulkner, S. Lin, and P. Rath, *Reflected entropy in random tensor networks III: triway cuts*, [arXiv:2409.17218](https://arxiv.org/abs/2409.17218).
- [52] P. Bueno and H. Casini, *Reflected entropy, symmetries and free fermions*, *JHEP* **05** (2020) 103, [[arXiv:2003.09546](https://arxiv.org/abs/2003.09546)].
- [53] P. Bueno and H. Casini, *Reflected entropy for free scalars*, *JHEP* **11** (2020) 148, [[arXiv:2008.11373](https://arxiv.org/abs/2008.11373)].
- [54] S. Dutta, T. Faulkner, and S. Lin, *The reflected entanglement spectrum for free fermions*, *JHEP* **02** (2023) 223, [[arXiv:2211.17255](https://arxiv.org/abs/2211.17255)].

[55] J. K. Basak, D. Giataganas, S. Mondal, and W.-Y. Wen, *Reflected entropy and Markov gap in non-inertial frames*, [arXiv:2306.17490](https://arxiv.org/abs/2306.17490).

[56] C. Berthiere, H. Chen, Y. Liu, and B. Chen, *Topological reflected entropy in Chern-Simons theories*, *Phys. Rev. B* **103** (2021), no. 3 035149, [[arXiv:2008.07950](https://arxiv.org/abs/2008.07950)].

[57] Y. Liu, R. Sohal, J. Kudler-Flam, and S. Ryu, *Multipartitioning topological phases by vertex states and quantum entanglement*, *Phys. Rev. B* **105** (2022), no. 11 115107, [[arXiv:2110.11980](https://arxiv.org/abs/2110.11980)].

[58] R. Sohal and S. Ryu, *Entanglement in tripartitions of topological orders: a diagrammatic approach*, [arXiv:2301.07763](https://arxiv.org/abs/2301.07763).

[59] Y. Kusuki and K. Tamaoka, *Dynamics of Entanglement Wedge Cross Section from Conformal Field Theories*, *Phys. Lett. B* **814** (2021) 136105, [[arXiv:1907.06646](https://arxiv.org/abs/1907.06646)].

[60] J. Kudler-Flam, Y. Kusuki, and S. Ryu, *Correlation measures and the entanglement wedge cross-section after quantum quenches in two-dimensional conformal field theories*, *JHEP* **04** (2020) 074, [[arXiv:2001.05501](https://arxiv.org/abs/2001.05501)].

[61] M. Moosa, *Time dependence of reflected entropy in rational and holographic conformal field theories*, *JHEP* **05** (2020) 082, [[arXiv:2001.05969](https://arxiv.org/abs/2001.05969)].

[62] J. Kudler-Flam, Y. Kusuki, and S. Ryu, *The quasi-particle picture and its breakdown after local quenches: mutual information, negativity, and reflected entropy*, *JHEP* **03** (2021) 146, [[arXiv:2008.11266](https://arxiv.org/abs/2008.11266)].

[63] C. Berthiere and G. Perez, *Reflected entropy and computable cross-norm negativity: Free theories and symmetry resolution*, *Phys. Rev. D* **108** (2023), no. 5 054508, [[arXiv:2307.11009](https://arxiv.org/abs/2307.11009)].

[64] C. Berthiere, B. Chen, and H. Chen, *Reflected entropy and Markov gap in Lifshitz theories*, *JHEP* **09** (2023) 160, [[arXiv:2307.12247](https://arxiv.org/abs/2307.12247)].

[65] C. Akers and P. Rath, *Entanglement Wedge Cross Sections Require Tripartite Entanglement*, *JHEP* **04** (2020) 208, [[arXiv:1911.07852](https://arxiv.org/abs/1911.07852)].

[66] P. Hayden, O. Parrikar, and J. Sorce, *The Markov gap for geometric reflected entropy*, *JHEP* **10** (2021) 047, [[arXiv:2107.00009](https://arxiv.org/abs/2107.00009)].

[67] P. Hayden, M. Lemm, and J. Sorce, *Reflected entropy: Not a correlation measure*, *Phys. Rev. A* **107** (2023), no. 5 L050401, [[arXiv:2302.10208](https://arxiv.org/abs/2302.10208)].

[68] S. D. Mathur, *The Information paradox: A Pedagogical introduction*, *Class. Quant. Grav.* **26** (2009) 224001, [[arXiv:0909.1038](https://arxiv.org/abs/0909.1038)].

[69] B. Collins, *Moments and cumulants of polynomial random variables on unitarygroups, the Itzykson-Zuber integral, and free probability*, *Int. Math. Res. Not.* **2003** (2003), no. 17 953–982.

- [70] B. Collins and P. Śniady, *Integration with Respect to the Haar Measure on Unitary, Orthogonal and Symplectic Group*, *Commun. Math. Phys.* **264** (2006), no. 3 773–795.
- [71] J. Chu, R. Qi, and Y. Zhou, *Generalizations of Reflected Entropy and the Holographic Dual*, *JHEP* **03** (2020) 151, [[arXiv:1909.10456](https://arxiv.org/abs/1909.10456)].